Applied Catalysis B: Environmental 129 (2013) 599–605

Contents lists available at SciVerse ScienceDirect

Applied Catalysis B: Environmental

journal homepage: www.elsevier.com/locate/apcatb

Photocatalytic reduction of carbon dioxide to formic acid, formaldehyde, and methanol using dye-sensitized TiO_2 film

Guohui Qin[a], Yue Zhang[a], Xuebin Ke[b], Xinli Tong[a], Zhe Sun[a], Mao Liang[a], Song Xue[a,*]

[a] School of Chemistry & Chemical Engineering, Tianjin University of Technology, Tianjin 300384, China
[b] School of Chemistry, Physics and Mechanical Engineering, Queensland University of Technology, Australia

ARTICLE INFO

Article history:
Received 7 August 2012
Received in revised form 9 October 2012
Accepted 14 October 2012
Available online 23 October 2012

Keywords:
Photocatalysis
Dye-sensitized TiO_2
CO_2 reduction
Electron transfer

ABSTRACT

A bifunctionalized TiO_2 film containing a dye-sensitized zone and a catalysis zone is designed for visible-light photocatalytic reduction of CO_2 to chemicals continuously. Charge separation can be accomplished with electron transferring to catalysis zone and positive charge transforming to anode. Highly efficient conversion of CO_2 to formic acid, formaldehyde, and methanol is achieved through the transferring electrons on conduction bands (CB) of TiO_2. Reduction of CO_2 and O_2 evolution take place in separated solutions on different catalysts. The separated solution carried out in this photo-reactor system can avoid CO_2 reduction products being oxidized by anode. The yields of reduction products were enhanced remarkably by external electrical power. This study provides not only a new photocatalytic system but also a potential of renewable energy source via carbon dioxide.

1. Introduction

Solar energy emerges as a clean, abundant and secure source to meet the demand for sustainable development. One of the most attractive means to storage energy in sunlight is the efficient conversion of solar energy to chemical energy. "Photosynthesis-to-Fuels" is described as utilizing CO_2, H_2O, and sunlight to form biomass, fuel H_2, and hydrocarbon chemicals [1–5]. Many efforts have been focused on photocatalytic conversion of CO_2 and H_2O to chemical fuels [6–20]. Among them, titanium dioxide (TiO_2) was extensively studied as a photocatalyst because of its high photocatalytic activity, long-term chemical stability, non-toxicity and low cost [21–26].

Electron (e^-) and hole (h^+) are generated in photolytic process using TiO_2 photocatalysts. The photo-excited electrons can reduce CO_2 to form CO, formic acid, methanol, and methane [27,28]. The holes can oxidize water to form $^\bullet$OH radicals in aqueous medium [29]. The formed $^\bullet$OH radicals and/or holes can also catalyze reverse reactions to oxidize the CO_2 reduction products e.g. methanol, which impede the reduction efficiency. Hole scavengers, such as 2-propanol, are often used to prevent electron–hole recombination and suppress the oxidation of these reduction products [30–32]. But these organic scavengers are consumable and unsustainable, for instance, 2-propanol is oxidized to propan-2-one, and even mineralized to CO_2 and H_2O. Furthermore, most of current photocatalysts, especially those modified by organic dyes and transition–metal complexes, suffer from poor stability due to severe oxidative stress for a long period of time, causing gradual loss of catalytic activity.

Dye-sensitized solar cells (DSCs) have received great attention since reported by Grätzel [33]. The basic functioning principle of the DSCs is similar to natural photosynthesis. In the first stage of plant photosynthesis, water molecules are photo-oxidized by chlorophyll to release oxygen and protons. The second stage of photosynthesis is a light-independent reaction in which carbon dioxide is converted to glucose. In DSCs, light absorption and charge separation are performed through a sandwich structure consisted of titanium oxide deposited on conducting glass, dye, electrolyte, and counter electrode [34,35]. Can the separated electrons in DSCs diffuse to catalytic active sites and induce chemical transformations there? This paper presents a new design using bifunctionalized TiO_2 film for photocatalytic reduction of CO_2 to formic acid, formaldehyde, and methanol locally.

The bifunctionalized TiO_2 film was designed to possess a dye-sensitized zone (namely DS zone) and a catalysis zone with a strategy to promote the separation, transfer, and renewing of photo-excited electrons (Scheme 1). The TiO_2 film was fabricated by adopting a non-conducting glass sheet instead of conducting glass (Fig. S1). The top half was coated with dye-sensitized TiO_2 film and another half was covered with purity TiO_2 film. The DS zone was composed of dye-sensitized TiO_2 film, electrolyte, and counter electrode. The catalysis zone had active sites to catalyze CO_2 reduction reactions. Electrons injected from dyes into conduction bands (CB) of TiO_2 in the DS zone can diffuse to the catalysis zone along the

* Corresponding author.
E-mail address: xuesong@ustc.edu.cn (S. Xue).

0926-3373/$ – see front matter © 2012 Elsevier B.V. All rights reserved.
http://dx.doi.org/10.1016/j.apcatb.2012.10.012

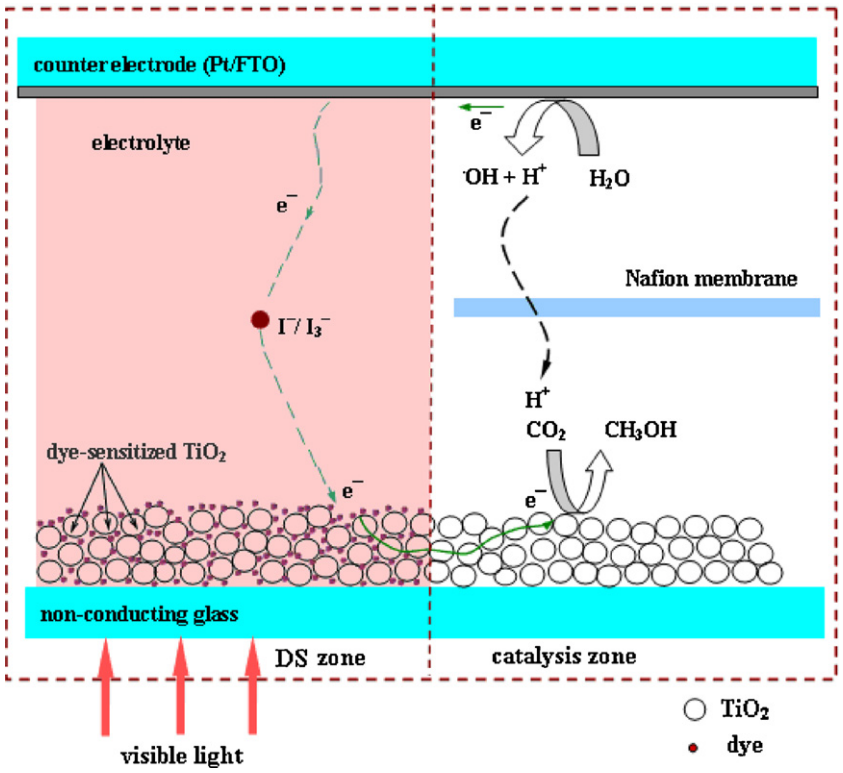

Scheme 1. Working mechanism for photocatalytic reduction of CO_2 using the bifunctionalized TiO_2 film.

network of TiO_2 nanoparticles, which has been confirmed by efficient degradation of phenols [36]. If TiO_2 film is deposited on a conducting glass, electrons would be trapped in conducting glass and become hard to transport from the conducting glass to the surface of semiconducting TiO_2 nanoparticles, leading to negligible degradations. The bifunctionalized TiO_2 film inspired us to conduct the photocatalytic reduction of CO_2 to chemical fuels via the electron transfer at CB of TiO_2, just like the second stage of photosynthesis in plant.

2. Experimental

2.1. Bifunctionalized TiO_2 film preparation

The bifunctionalized TiO_2 film was fabricated according to our previous report [35]. TiO_2 colloid was prepared according to the literature method [39], which was used for the preparation of the nanocrystalline films. The TiO_2 paste was firstly prepared using ethyl cellulose as a binder and terpineol as a solvent, which consisted of 18 wt% TiO_2, 9 wt% ethyl cellulose and 73 wt% terpineol. The TiO_2 paste was deposited on a non-conductive glass sheet by screen printing. The thickness of the TiO_2 film was controlled by repetition of printing. The film was dried in air at 120 °C for 30 min and calcined at 500 °C for 30 min under flowing oxygen before cooling to room temperature. A area of TiO_2 film (14 mm × 14 mm) with *ca.* 5 μm thickness was stained by immersing it into a dye solution containing 300 μM bis(tetrabutylammonium)-*cis*-bis(isothiocyanato) bis(2,2′-bipyridyl-4,4′-dicarboxylato)-ruthenium(II) (N719) as dye sensitizer (Scheme S1), which is among the best photosensitizers used in mesoporous TiO_2-based dye sensitized solar cells (DSCs). The formed surface complex with TiO_2 is stabilized via a combination of bidentate-bridging and H-bonding [40]. After 24 h at room temperature, the dye-stained film was rinsed with dry ethanol and dried by a dry air flow. Pt was deposited on FTO glass (16 mm × 18 mm, Nippon Sheet Glass, Hyogo, Japan, fluorine doped SnO_2, sheet resistance 10 Ω/square, transmission >90% in the visible) by coating with a drop of H_2PtCl_6 solution (40 mM in ethanol) with heat treatment at 395 °C for 15 min to give a counter electrode. The dye-sensitized TiO_2 film and counter electrode were separated by a surlyn spacer film (50 μm thick) and sealed by heating to form a sandwich type cell. Electrolyte was then injected into the cell gap to form the bifunctionalized TiO_2 film. The electrolyte was a solution of 0.6 M 1,2-dimethyl-3-n-propylimidazolium iodide (DMPImI), 0.1 M LiI, 0.05 M I_2, and 0.5 M 4-tert-butylpyridine in acetonitrile. The non-dye-sensitized TiO_2 film, namely catalysis zone, was used for catalytic reaction sites. Therefore, the bifunctionalized TiO_2 film with a dye-sensitized zone (DS zone) and a catalysis zone was fabricated. The two zones had the same area of TiO_2 film (14 mm × 14 mm).

2.2. Photocatalytic reaction and measurements

A 300 W Xe lamp (L25, λ_{max} = 500 nm) was used as the visible light source, which irradiated at a distance of 20 cm to the TiO_2 film surface through 420 nm cutoff filters. The CO_2 reduction experiment was conducted in H-type reactor with 50 mL of distilled water in each solution (Fig. 1). The catalysis zone with an activated area of 1.96 cm^2 was inserted into solution **I**. An electrode (Pt/FTO) with the same area acted as anode was inserted into solution **II**. The two solutions were separated by Nafion membrane. The counter electrode of the DS zone is connected with the anode through a copper wire. The initial pH in solution was adjusted by 2 M NaOH or 2 M H_2SO_4. CO_2 was bubbled into the solution **I** through a pipe. After bubbling for 10 min, light irradiation was started, and CO_2 was bubbled continuously at a rate of 10 L/h during the reaction. The concentration of formic acid was determined by a HPLC using an Agilent 1100 chromatograph equipped with a ZORBAX Eclipse XDB-C18 reversed phase column. The yield of formaldehyde was determined with UV–vis spectrophotometer. The concentration of methanol

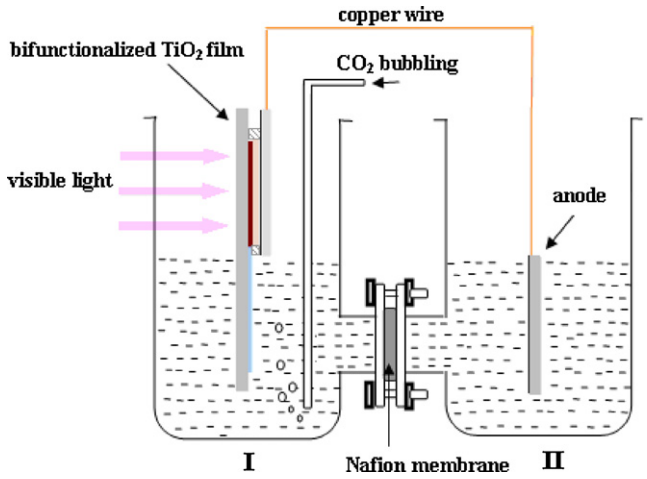

Fig. 1. Photocatalytic reduction of carbon dioxide in H-type reactor.

was determined by a GC/FID. Yields of formic acid, formaldehyde, and methanol are calculated based on the amounts of products per area of 14 mm × 14 mm.

3. Results and discussion

The CO_2 reduction experiment was conducted in the H-type reactor (Fig. 1). The initial pH in solution was adjusted to 10 by 2 M NaOH. As seen from Fig. 2, the formation of formic acid, formaldehyde, and methanol is observed with yields of 0.0835, 0.1292, and 0.1781 mmol cm^{-2}, respectively, after visible light illumination for 5 h. The yields of formaldehyde and methanol increase with illumination time. But the formation rate of formic acid increases to the maximum at t = 3 h, then starts to decline. It may be attributed to the competitive reductions of CO_2 and formic acid. In a series of reductions, CO_2 is firstly converted into formic acid, then formaldehyde and methanol. Electrons are needed for each step of conversion. The increase in the yields of formic acid and formaldehyde with illumination time will cause an increase in the consumption of electrons as well, leading to the declining of available electrons for conversion of CO_2 to formic acid. This is largely because reduction of formic acid and formaldehyde is easier than conversion of CO_2 to formic acid. These CO_2 reduction products in aqueous solution are further confirmed by GC–MS spectra as shown in Supporting Information.

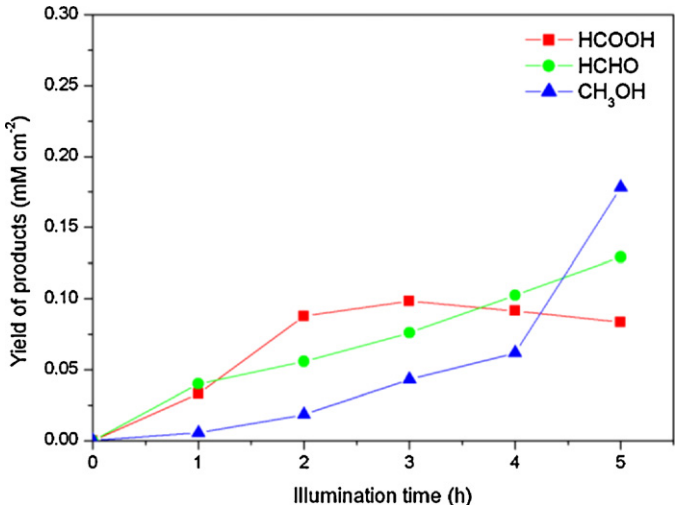

Fig. 2. Yields of CO_2 reduction products under conditions: light > 420 nm, CO_2 10 L/h, activated area 1.96 cm^2, pH 10.

The results demonstrate that using the bifunctionalized TiO_2 film, CO_2 can be converted to formic acid, formaldehyde, and methanol under visible light irradiation.

It is well known that, for photocatalytic reduction of CO_2 in aqueous solution, if oxidation and reduction reactions occur on the same catalyst surface, it will result in interactions between the surface adsorbates, which are inhibitory on the reduction reaction. In addition, charges presented on semiconductor and/or doped metal surface in an uncontrolled mode increase the chance of charge recombination. In the design of our reaction system, the reduction reaction takes place in solution **I** through electrons at surface of TiO_2 film in catalysis zone, whereas the oxidation reaction occurs in solution **II** by positive charges on Pt catalyst at anode. The separation of oxidation reaction from reduction reaction prevents the interactions of surface adsorbates from taking placer. In the meantime, charges separated through controlled DSCs structure design can suppress charge recombination. Beside the use of two different catalysts, the oxidation and reduction reactions should be carried out in separated solution. Otherwise, the yields of CO_2 reduction products would be significantly lower. For example, when the CO_2 reduction experiment was conducted in a wide-mouth glass flask reactor with the bifunctionalized TiO_2 film and anode inserted (Fig. S2), after illuminating for 5 h, formic acid, formaldehyde, and methanol were achieved with yields of 0.0511, 0.0644, and 0.0612 mmol cm^{-2}, respectively (Fig. S3). The yield of methanol obtained in separated solution was nearly three times as that in unseparated solution (0.1781 versus 0.0612 mmol cm^{-2}). These results show that the anode inserted in reduction solution exerts a negative effect on the CO_2 reduction. The oxidation of anode favors degradation of organic products derived from CO_2, leading to a low yield of reduction products. As a result, for photocatalytic CO_2 conversion, the photoinduced hole/positive charge (h^+) should be isolated from the reduction system to avoid further oxidization of reduction products. Meanwhile, catalytically functionalized anode is crucial for the continuous conversion of CO_2 in our system. In the absence of anode while only using bifunctionalized TiO_2 film, the reduction of CO_2 will proceed for a short period of time, then will cease gradually.

As shown in Scheme 1, electron is injected into CB of TiO_2 in DS zone by light excitation and dye is oxidized to dye^+. The injected electrons diffuse from the DS zone to the catalysis zone through the network of TiO_2 nanoparticles, and react with CO_2 to produce chemical fuels. On the other hand, the oxidized dye is regenerated by stripping electron from I^- in electrolyte, oxidizing it into I_3^-. If there is no electron supplied for recovering I^- from I_3^-, the concentration of I^- in electrolyte would decrease gradually and eventually disappeared, leading to the termination of CO_2 reduction reaction. In this study, the electron is derived from water oxidation activated by anode. When I_3^- is catalytically converted into I^- through counter electrode with electron exchange, the positive charge is transported from counter electrode to anode through copper wire. As dyes repeated the process cycle of light absorption and regeneration, the oxidation potential of anode becomes high enough for water oxidation, producing $^{\bullet}OH/O_2$, proton, and electron. Protons are transferred through Nafion membrane to take part in CO_2 conversion. The released electrons are afforded for conversion of I_3^- into I^-. At the beginning of photocatalytic reaction, the source of electron for CO_2 reduction is derived from I^- in electrolyte. Due to the anodic oxidation for electron release, water eventually becomes the source of electron for I^-/I_3^- redox cycle.

In our original design, the regeneration of electrons relies on the electron release from water taking place on anode. To clarify the reaction mechanism, an approach was introduced to enhance this electron regeneration process by supplying all the electrons required for conversion of I_3^- into I^-. An external voltage using a DC power source was applied in the photocatalytic reduction

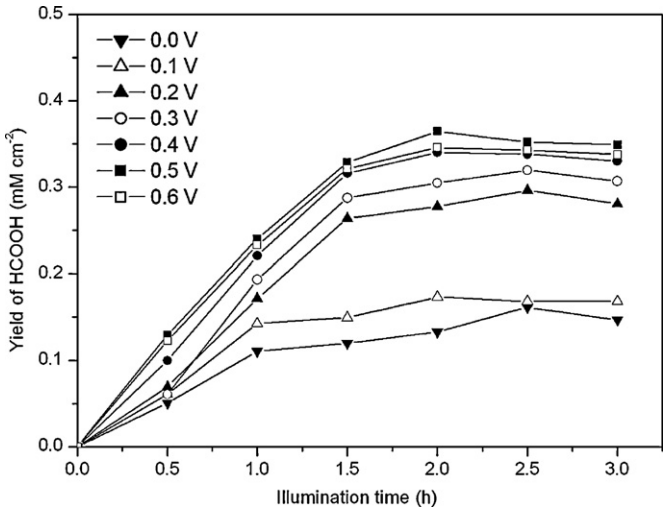

Fig. 3. Effect of external voltage on the yield of formic acid under conditions: light > 420 nm, CO_2 10 L/h, activated area 1.96 cm^2, pH 10, external power.

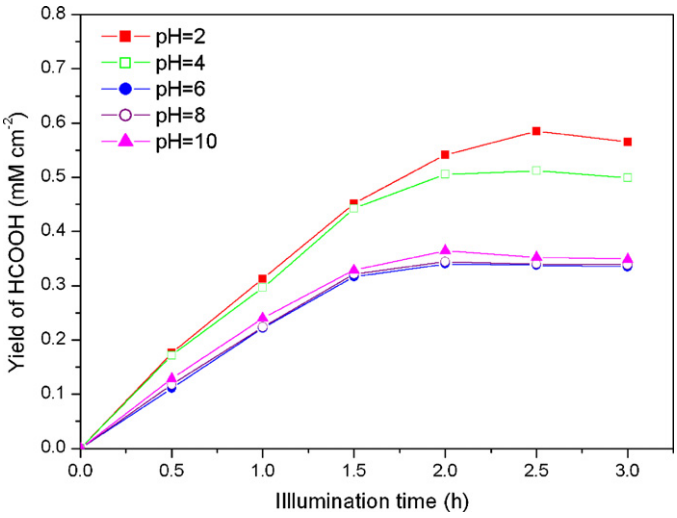

Fig. 4. Effect of pH on the yield of formic acid under conditions: light > 420 nm, CO_2 10 L/h, activated area 1.96 cm^2, external voltage 0.5 V.

reaction. The negative pole of power source was connected to the counter electrode, while the positive electrode was connected with the anode. The effect of using external DC power was studied under the voltages of 0.6, 0.5, 0.4, 0.3, 0.2, 0.1, and 0.0 V. As shown in Fig. 3, the yield of formic acid is increased when voltage is changed from 0.0 to 0.5 V. A yield of 0.364 mmol cm^{-2} for formic acid is obtained at a voltage of 0.5 V after 2 h, whereas only 0.0878 mmol cm^{-2} is obtained without external voltage. The yield of formaldehyde increases obviously when external voltage is supplied from 0.0 to 0.5 V (Fig. S4). The formation of methanol increases gradually with illumination time then continues to increase sharply over 2 h (Fig. S5). The sharp increase in the yield of methanol after 2 h is due to the high concentration of formed formaldehyde. At the starting reaction time, the yields of formic acid and formaldehyde increased obviously with reaction time, while methanol was formed with low yield due to the comparable low concentration of formaldehyde. About 2 h later, formic acid and formaldehyde reached high concentrations, and their yields did not increase any more with reaction time. High concentration of formaldehyde promoted the formation of methanol. In addition, among the observed products (HCOOH, HCHO, and CH_3OH), there is little change in the concentrations of HCOOH and HCHO after 2 h, which means that photoelectrons convert CO_2 to methanol in net reactions via the formation of HCOOH and HCHO. These results cause a sharply increasing yield of methanol. Compared with the yield of 0.1781 mmol cm^{-2} obtained in absence of external voltage (t = 5 h), a higher yield of 0.295 mmol cm^{-2} is achieved at voltage of 0.5 V at shorter time (t = 3 h). The excellent yields of CO_2 reduction promoted by using DC power are attributed to the following reasons. The negative pole of DC power source connected to the counter electrode supplies abundant electrons from the power supplier for the conversion of I_3^- to I^-. The enrichment of I^- enables regeneration of the oxidized dyes immediately. The acceleration in regeneration of dyes produces much more electrons which are injected into the conduction bands of TiO_2 under light irradiation. Enhanced electron supply leads to higher yields of CO_2 reduction products. For comparison, experiments of CO_2 reduction performed in the dark conditions show no appearance of formic acid, formaldehyde, and methanol, even at a voltage of 0.5 V, proving that the reduction reaction of CO_2 is driven by light, not by electric power.

The reduction reaction of CO_2 to formic acid, formaldehyde and methanol at different initial pH was illustrated in Figs. 4, S6, and 5 respectively. The variation of pH had an obvious influence on the yields of those compounds. Higher yields were obtained when experiments were performed in acidic solutions than in alkaline solutions. For example, formic acid was observed with a yield of 0.585 mmol cm^{-2} at pH 2, whereas only a yield of 0.364 mmol cm^{-2} at pH 10. The similar effect was also found in the formation of formaldehyde. It is noted that methanol yield is higher at pH 10 than that at pH 6 and 8, which might be a pH effect and/or an ionic strength effect. To test the effect of ionic strength on yield of methanol, experiments were carried out under salt solution containing 0.5 M Na_2SO_4 at pH 7 and 10. As shown in Fig. 5, in the case of salt solution, methanol was obtained with higher yield at pH 10 than that at pH 7. This result is in consistent with that in no-salt solution. On the other hand, at pH 10, reaction performed in no-salt solution give a higher yield of methanol than that in salt solution. These results show that pH has an obvious influence on the formation of product, and ionic salt has an imperceptible effect on yields. The little ionic strength effect might be attributed to the photocatalytic reaction rather than the electrochemical process.

The process mechanism for photocatalytic reduction of carbon dioxide in aqueous solution has been proposed in the literature reports [37,38]. To verify the pathway for the formation of these compounds, two experiments were carried out. One is that CO_2

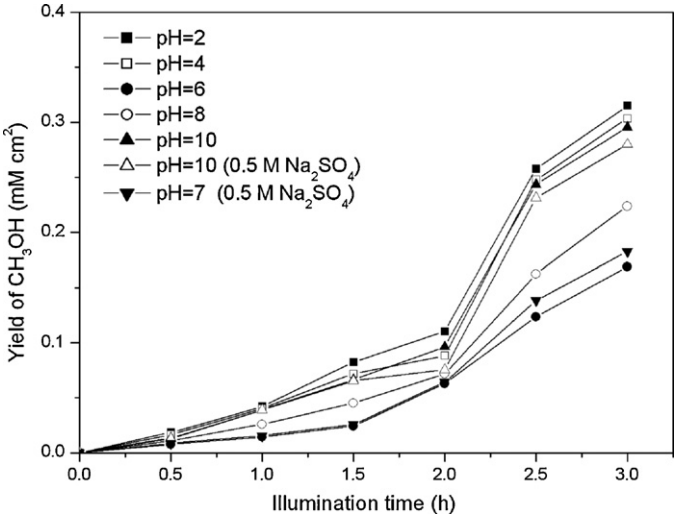

Fig. 5. Effect of pH on the yield of methanol under conditions: light > 420 nm, CO_2 10 L/h, activated area 1.96 cm^2, external voltage 0.5 V.

In acidic solution

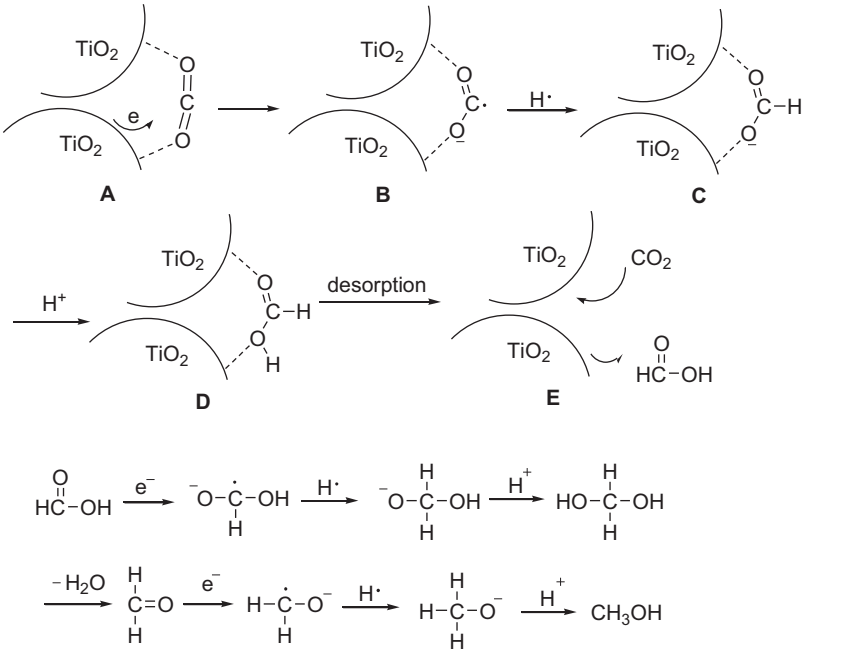

In alkaline solution

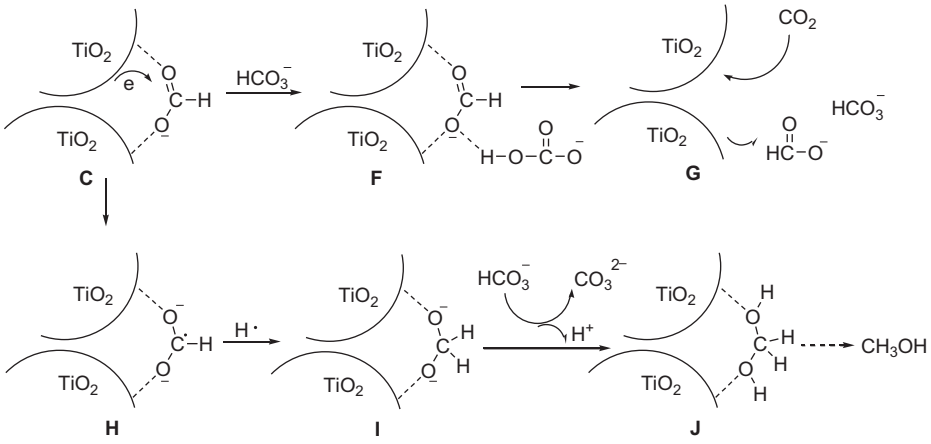

Scheme 2. Possible mechanism for reduction of CO_2 to formic acid, formaldehyde, and methanol.

was bubbled at the first 1 h, then bubbling stopped in next 2 h. As shown in Fig. 6, the yield of formic acid turned from an increase into a decrease over 1 h although small amount of CO_2 was dissolved in solution after bubbling CO_2 stopped. The reaction rate for formation of formic acid would become slow when bubbling CO_2 stopped. But conversion of formic acid to formaldehyde was continuous, resulting in a decrease of formic acid after 1 h. The yield of methanol increased gradually with illumination time, which suggests that methanol is produced from formaldehyde or formic acid, not directly from CO_2. It is found that when bubbling CO_2 stopped after one hour, methanol was obtained with a higher yield than that of continuously bubbling CO_2. Reduction of CO_2 to formic acid, formaldehyde, and methanol need electrons in each step of conversion. When bubbling CO_2 stops, the concentration of CO_2 in solution decreases gradually, leading to less electrons used for conversion of CO_2 to formic acid. More saved electrons will take part in the conversion of formaldehyde to methanol and afford larger amount of methanol. The other experiment was carried out at initial solution containing 0.277 mmol cm^{-2} formic acid and no bubbling CO_2 all the time. The concentration of formic acid decreased with illumination time (Fig. S7). The formation of formaldehyde and methanol was observed and increased gradually. After 2 h, yield of formaldehyde decreased, whereas methanol was on continuous increase. These results clearly demonstrate that the bifunctionalized TiO_2 film can convert formic acid to formaldehyde, and further to methanol under light irradiation.

Considering the practical application, the durability of the bifunctionalized TiO_2 film was tested in relatively large reactor volume of 500 mL of distilled water under illumination for 30 h. As shown in Fig. 7, the yields of formaldehyde and methanol increase with illumination time. Whereas the yield of formic acid increases initially, then decreases slightly after 25 h, which is similar to the result shown in Fig. 2. The formation of these products from CO_2 demonstrates that as-prepared bifunctionalized TiO_2 film is relatively stable under the studied conditions. It has great potential to proceed actual sunlight testing.

A possible mechanism for reduction of CO_2 to formic acid, formaldehyde, and methanol is shown in Scheme 2. CO_2 (O=C=O)

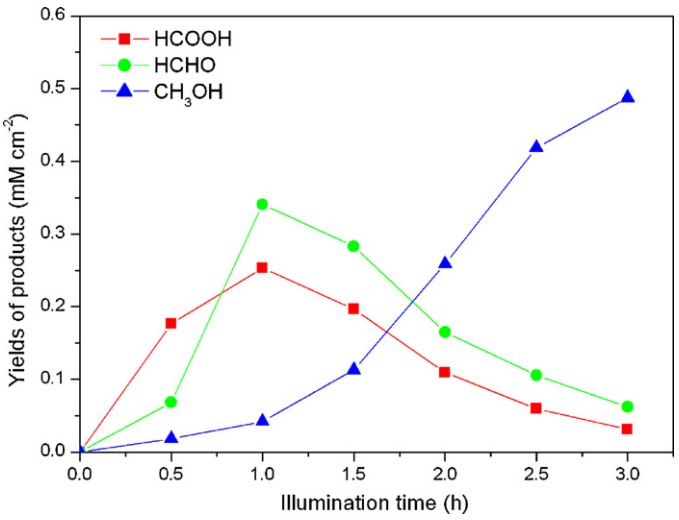

Fig. 6. Yields of CO_2 reduction products when CO_2 was bubbled at the first 1 h, then bubbling stopped in next 2 h under conditions: light > 420 nm, activated area 1.96 cm^2, pH 2, external voltage 0.5 V.

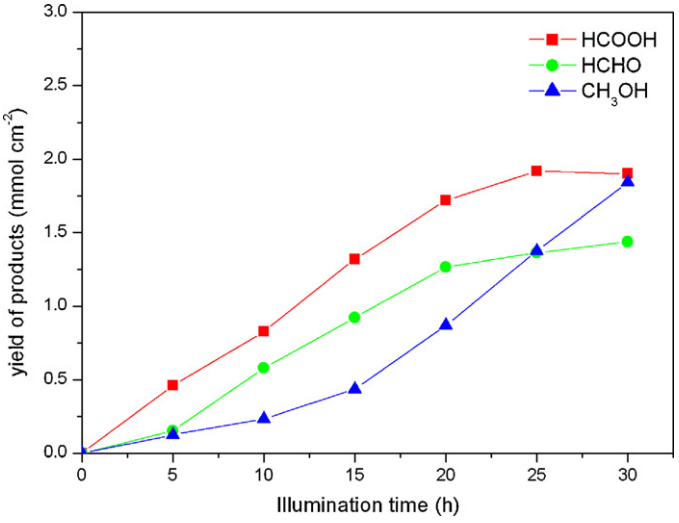

Fig. 7. Yields of CO_2 reduction products within 30 h under conditions: light > 420 nm, activated area 1.96 cm^2, pH 2.

is first absorbed on TiO_2 nanoparticles surface, and becomes a distorted molecular (**A**). The C=O bond of CO_2 becomes long and its π-bond is activated. Then the activated C=O bond is attacked by an electron from the conduction band of TiO_2 to form $C^{\bullet}$—O^- (**B**). Reaction of H^+ with an electron generates $^{\bullet}H$. The intermediate $CO_2^{\bullet-}$ by reaction with $^{\bullet}H$ is transformed into $HCOO^-$ (**C**). If reaction is under acidic conditions, H^+ ion can interact with $HCOO^-$ to give absorbed HCOOH (**D**). Formic acid is desorbed from nanoparticles surface, and release vacant site for absorbing another CO_2. The absorbed HCOOH (**D**) can be further reduced to HCHO and CH_3OH. If reaction is in alkaline solution, the solution contains species HCO_3^- and CO_3^{2-} through bubbling CO_2. In comparison with pH = 8, higher pH value (pH = 10) will produce higher concentration of these two species. The HCO_3^- ion interacts with $HCOO^-$ to desorb $HCOO^-$ from nanoparticles surface to give **G**. Because of alkaline solution, the intermediate **F** is not easily converted to **G**, leading to lower yield of formic acid compared with acidic solution. The absorbed $HCOO^-$ of the intermediate **C** prefers to attack by another electron to form **H**, followed by reaction with $^{\bullet}H$ and HCO_3^- to give intermediate **J**. The intermediate **J** affords HCHO through elimination of H_2O, and further reduced to CH_3OH. Therefore, $HCOO^-$ and HCHO are not easily desorbed from nanoparticles surface in alkaline solution. They are unceasingly reduced to methanol, which cause it with high yield at pH 10.

4. Conclusions

The bifunctionalized TiO_2 film was designed to facility the electron separation in DS zone, the electron transition from DS zone to catalysis zone, and renewing from the anode. The products of formic acid, formaldehyde and methanol are obtained through the high efficiency photo-reactor system. The anode in separated solution avoids these obtained products being oxidized. The yields of products from CO_2 conversion were enhanced remarkably by an external electrical power. The presented results afford a highly promising platform for realization of carbon renewable energy cycle under sunlight.

Acknowledgments

We are thankful to Professor Jianli Hu for his beneficial discussion in preparation of this paper. This work is supported by the National Natural Science Foundation of China (21072152, 21101115).

Appendix A. Supplementary data

Supplementary data associated with this article can be found, in the online version, at http://dx.doi.org/10.1016/j.apcatb.2012.10.012.

References

[1] A. Melis, Energy & Environmental Science 5 (2012) 5531–5539.
[2] S. Bensaid, G. Centi, E. Garrone, S. Perathoner, G. Saracco, S. Bensaid, G. Centi, E. Garrone, S. Perathoner, G. Saracco, ChemSusChem 5 (2012) 500–521.
[3] J. Barber, Chemical Society Reviews 38 (2009) 185–196.
[4] V. Artero, M. Chavarot-Kerlidou, M. Fontecave, Angewandte Chemie International Edition 50 (2011) 7238–7266.
[5] S. Chrsitopher, P. Linic, D.B. Ingram, Nature Materials 10 (2011) 911–921.
[6] Y. Li, W.N. Wang, Z. Zhan, M.-H. Woo, C.-Y. Wu, P. Biswas, Applied Catalysis B: Environmental 100 (2010) 386–392.
[7] S. Vasireddy, B. Morreale, A. Cugini, C.S. Song, J.J. Spivey, Energy & Environmental Science 4 (2011) 311–345.
[8] S. Matsuoka, K. Yamamoto, T. Ogata, M. Kusaba, N. Nakashima, E. Fujita, S. Yanagida, Journal of the American Chemical Society 115 (1993) 601–609.
[9] M. Cokoja, C. Bruckmeier, B. Rieger, W.A. Herrmann, E.F. Kühn, Angewandte Chemie International Edition 50 (2011), 8510-8137.
[10] M.D. Doherty, D.C. Grills, J.T. Muckerman, D.E. Polyansky, E. Fujita, Coordination Chemistry Reviews 254 (2010) 2472–2482.
[11] E.E. Benson, C.P. Kubiak, A.J. Sathrum, J.M. Smieja, Chemical Society Reviews 38 (2009) 89–99.
[12] A.J. Morris, G.J. Meyer, E. Fujita, Accounts of Chemical Research 42 (2009) 1983–1994.
[13] G.D. Scholes, G.R. Fleming, A. Olaya-Castro, R. van Grondelle, Nature Chemistry 3 (2011) 763–774.
[14] W.Y. Lin, H. Frei, Journal of the American Chemical Society 127 (2005) 1610–1611.
[15] C.J. Wang, R.L. Thompson, J. Baltrus, C. Matranga, Journal of Physical Chemistry Letters 1 (2010) 48–53.
[16] T.M. Suzuki, H. Tanaka, T. Morikawa, M. Iwaki, S. Sato, S. Saeki, M. Inoue, T. Kajino, T. Motohiro, Chemical Communications 47 (2011) 8673–8675.
[17] S.C. Roy, O.K. Varghese, M. Paulose, C.A. Grimes, Nano 4 (2010) 1259–1278.
[18] J.C.S. Wu, H. Lin, C.L. Lai, Applied Catalysis A: General 296 (2005) 194–200.
[19] Z.Y. Wang, H.C. Chou, J.C.S. Wu, D.P. Tsai, G. Mul, Applied Catalysis A 380 (2010) 172–177.
[20] Z. Zou, J. Ye, H. Arakawa, Chemical Physics Letters 332 (2000) 271–277.
[21] Z.W. Liu, W.B. Hou, P. Pavaskar, M. Aykol, S.B. Cronin, Nano Letters 11 (2011) 1111–1116.
[22] S.T. Hussain, K. Khan, R. Hussain, Journal of Natural Gas Chemistry 18 (2009) 383–473.
[23] K. Koci, L. Matejova, L. Obalova, S. Krejckov, Z. Lacny, D. Placha, L. Capek, A. Hospodkovad, O. Solcova, Applied Catalysis B: Environmental 96 (2010) 239–244.
[24] O. Ozcan, F. Yukruk, E.U. Akkaya, D. Uner, Topics in Catalysis 44 (2007) 523–528.
[25] K.R. Thampi, J. Kiwi, M. Graetzel, Nature 327 (1987) 506–508.

[26] W.B. Hou, W.H. Hung, P. Pavaskar, A. Goeppert, M. Aykol, S.B. Cronin, ACS Catalysis 1 (2011) 929–936.
[27] M. Anpo, K. Chiba, Journal of Molecular Catalysis 74 (1992) 207–212.
[28] M. Halmann, M. Ulman, B.A. Blajeni, Solar Energy 31 (1983) 429–431.
[29] C.D. Jaeger, A.J. Bard, Journal of Physical Chemistry 83 (1979) 3146–3152.
[30] S. Kaneco, Y. Shimizu, K. Ohta, T. Mizuno, Journal of Photochemistry and Photobiology A: Chemistry 115 (1998) 223–226.
[31] W. Choi, M.R. Hoffmann, Environmental Science and Technology 31 (1997) 89–95.
[32] F. Gartner, S. Losse, A. Boddien, M.-M. Pohl, S. Denurra, H. Junge, M. Beller, ChemSusChem 5 (2012) 530–533.
[33] B. O'Regan, M. Grätzel, Nature 353 (1991) 737–740.
[34] A. Hagfeldt, M. Grätzel, Accounts of Chemical Research 33 (2000) 269–277.
[35] R.E. Blankenship, D.M. Tiede, J. Barber, G.W. Brudvig, G. Fleming, M. Ghirardi, M.R. Gunner, W. Junge, D.M. Kramer, A. Melis, T.A. Moore, C.C. Moser, D.G. Nocera, A.J. Nozik, D.R. Ort, W.W. Parson, R.C. Prince, R.T. Sayre, Science 332 (2011) 805–809.
[36] G.H. Qin, Z. Sun, Q.P. Wu, L. Lin, M. Liang, S. Xue, Journal of Hazardous Materials 192 (2011) 599–604.
[37] S.S. Tan, L. Zou, E. Hu, Catalysis Today 115 (2006) 269–277.
[38] M. Anpo, H. Yamashita, Y. Ichihashi, S. Ehara, Journal of Electroanalytical Chemistry 396 (1995) 21–26.
[39] S. Ito, T.N. Murakami, P. Comte, P. Liska, C. Grätzel, M.K. Nazeeruddin, M. Grätzel, Thin Solid Films 516 (2008) 4613–4619.
[40] K.E. Lee, M.A. Gomez, S. Elouatik, G.P. Demopoulos, Langmuir 26 (2010) 9575–9583.